TWO LOCAL VOLUME DWARF GALAXIES DISCOVERED IN 21 CM EMISSION

Erik J. Tollerud[1,5], Marla C. Geha[1] Jana Grcevich[2,6], Mary E. Putman[3], Daniel Stern[4]
Draft version November 2, 2014

ABSTRACT

We report the discovery of two dwarf galaxies from a blind 21 cm H I search. The two galaxies were the only two galaxies found via optical imaging and spectroscopy of 22 H I clouds identified in the GALFA-HI survey as dwarf galaxy candidates. They have properties consistent with being in the Local Volume (< 10 Mpc), and one has resolved stellar populations such that it may be on the outer edge of the Local Group (~ 1 Mpc from M31). While the distance uncertainty makes interpretation ambiguous, these may be among the faintest starforming galaxies known. Additionally, rough estimates comparing these galaxies to ΛCDM dark matter simulations suggest consistency in number density, implying that dark matter halos likely to host these galaxies are primarily H I-rich. The galaxies may thus be indicative of a large population of dwarfs at the limit of detectability that are comparable to the faint satellites of the Local Group. Because they are outside the influence of a large dark matter halo to alter their evolution, these galaxies can provide critical anchors to dwarf galaxy formation models.

Subject headings: galaxies: dwarf — galaxies: individual (Pisces A, B) — radio lines: galaxies — Local Group

1. INTRODUCTION

The properties of faint dwarf galaxies at or beyond the outer reaches of the Local Group ($1 - 5$ Mpc) probe the efficiency of environmentally driven galaxy formation processes and provide direct tests of cosmological predictions (e.g. Klypin et al. 1999; Moore et al. 1999; Strigari et al. 2008; Kravtsov 2010; Kirby et al. 2010; Boylan-Kolchin et al. 2011; Pontzen & Governato 2012; Geha et al. 2013). However, searches for faint galaxies suffer from strong luminosity and surface brightness biases that render galaxies with $L_V \lesssim 10^6 \, L_\odot$ difficult to detect beyond the Local Group (Tollerud et al. 2008; Walsh et al. 2009; Hargis et al. 2014). Because of these biases, searching for nearby dwarf galaxies with methodologies beyond the standard optical star count methods are essential.

This motivates searches for dwarf galaxies using the 21 cm emission line of neutral hydrogen (H I). While such searches cannot identify passive dwarf galaxies like most Local Group satellites, which lack H I (Grcevich & Putman 2009; Spekkens et al. 2014), they have the potential to find gas-rich, potentially starforming dwarf galaxies. This is exemplified by the case of the Leo P dwarf galaxy, found first in H I and later confirmed via optical imaging (Giovanelli et al. 2013; Rhode et al. 2013).

[1] Astronomy Department, Yale University, P.O. Box 208101, New Haven, CT 06510, USA; erik.tollerud@yale.edu, marla.geha@yale.edu
[2] Department of Astrophysics, American Museum of Natural History, Central Park West at 79th St., New York, NY 10024, USA; jgrcevich@amnh.org
[3] Department of Astronomy, Columbia University, New York, NY 10027, USA; mputman@astro.columbia.edu
[4] Jet Propulsion Laboratory, California Institute of Technology, 4800 Oak Grove Drive, Mail Stop 169-221, Pasadena, CA 91109, USA; daniel.k.stern@jpl.nasa.gov
[5] Hubble Fellow
[6] Visiting Astronomer, Kitt Peak National Observatory, National Optical Astronomy Observatory, which is operated by the Association of Universities for Research in Astronomy (AURA) under cooperative agreement with the National Science Foundation.

Here we describe two faint dwarf galaxies identified via H I emission in the first data release of the Galactic Arecibo L-band Feed Array H I (GALFA-HI) survey (Peek et al. 2011). As described below, they are likely within the Local Volume (< 10 Mpc) but just beyond the Local Group ($\gtrsim 1$ Mpc), so we refer to them as Pisces A and B. This paper is organized as follows: in Section 2, we present the data used to identify these galaxies. In Section 3, we consider possible distance scenarios, while in Section 4 we provide context and some conclusions. Where relevant, we adopt a Hubble constant of $H_0 = 69.3 \, \mathrm{km \, s^{-1} Mpc^{-1}}$ from WMAP9 (Hinshaw et al. 2013).

2. DATA

The two galaxies we report on here were identified initially as cold H I clouds with possibly galaxy-like properties in DR1 of the GALFA-HI survey (Peek et al. 2011). Confirmation of these clouds as galaxies required additional optical imaging and spectroscopy, which we briefly describe below.

2.1. *H I Detection*

GALFA-HI was performed with the Arecibo Observatory 305 m telescope, using the ALFA feed array and the GALSPECT spectrometer. GALFA-HI DR1 (Peek et al. 2011) includes velocities $|V_{\mathrm{LSR}}| < 650 \, \mathrm{km \, s^{-1}}$, covers 7520 square degrees of sky from $\delta = -1°$ to $+38°$, has a channel spacing of $0.2 \, \mathrm{km \, s^{-1}}$, and a spatial resolution of $4'$. The sensitivity of DR1 varies with position, but the majority of the objects cataloged would have $M_{\mathrm{HI}} < 10^6 \, M_\odot$ if at $1 \, \mathrm{Mpc}$. The two candidate dwarfs were first found in a GALFA-HI DR1 catalog that identified H I clouds with sizes $< 20'$ and velocity FWHMs $< 35 \, \mathrm{km \, s^{-1}}$ (Saul et al. 2012). From the Saul et al. (2012) sample of 1964 clouds, Grcevich (2013) identified 51 candidate galaxies with fluxes and sizes similar to the known Local Group dwarf galaxies with gas

(particularly Leo T). The two candidates presented here were also identified by Saul et al. (2012) as being likely galaxies because they cannot be easily associated with known high velocity cloud (HVC) complexes or Galactic gas in position-velocity space.

2.2. *Optical Imaging*

We performed follow-up optical imaging of 22 of the H I clouds. These observations were performed with the pODI instrument on the WIYN Telescope[7] in the g and r-band filters, with integration times of 600-1200 sec per filter per target. Standard imaging reductions were performed by the ODI Portal, Pipeline, and Archive facility. These include bias subtraction, flat-fielding, and alignment of individual Orthogonal Transfer Array (OTA) cells into chips. The SWarp program (Bertin et al. 2002) was used to combine the individual exposures, and DAOPHOT (Stetson 1987) was used to perform PSF-fitting photometry on stars in the field.

Most of the H I clouds did *not* have optical counterparts with morphologies like nearby galaxies within the $\sim 4'$ GALFA-HI beam. Those in the Sloan Digital Sky Survey (SDSS, Ahn et al. 2014) footprint show neither diffuse features like the galaxies described below, nor point source overdensities to the limit of the DR 10 catalog. Similarly, our deeper pODI imaging showed neither overdensities nor Red Giant Branch (RGB) features in the color-magnitude diagrams (CMD) down to $r \lesssim 24$ (an RGB tip distance $> 3\,\mathrm{Mpc}$) for any of the targets we observed other than the two described below.

Only two objects showed dwarf galaxy-like overdensities of point sources within the GALFA-HI beam. These two candidate are shown in Figure 1. They are also visible in the SDSS, although the SDSS catalog incompletely deblends them into a mix of stars and galaxies. The morphology in these images is consistent with both objects being dwarf (irregular) galaxies. Additionally, the presence of such point sources resolved in ground-based imaging implies that the galaxies are relatively nearby ($\lesssim 10$ Mpc). In particular, Pisces A (left panel of Figure 1) shows point sources resolved enough to generate a CMD. We discuss this further in Section 3 in the context of providing a distance estimate.

2.3. *Optical Spectroscopy*

To confirm that the galaxies visible in Figure 1 correspond to the H I clouds discussed in Section 2.1, we observed both galaxies in twilight with the Double Spectrograph on the Palomar Hale 200 inch telescope on UT 2014 February 6. The observations were wavelength calibrated, bias- and sky-subtracted using standard longslit techniques. We show these spectra in Figure 2, with the lower panels showing the wavelengths near Hα and the upper panels displaying the H I emission.

The optical spectra reveal Hα emission, which we fit with Gaussian profiles. The central velocity of these lines are offset from the H I by only 3 ± 34 and $10 \pm 35\,\mathrm{km\,s^{-1}}$ (see Table 1), well within the Hα 1σ uncertainties. This demonstrates that the optical galaxies are indeed associated with the H I clouds. Because flux calibra-

tion was not possible for these observations due to non-photometric conditions, we cannot quantify the magnitude of star formation implied by the emission. However, the presence of detectable Hα emission implies star formation is ongoing in these galaxies, although at a lower level in Pisces A.
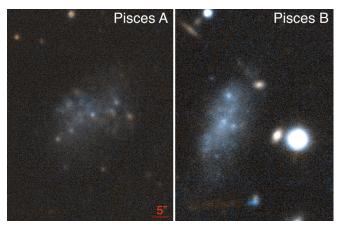

FIG. 1.— gr color composite images of dwarfs Pisces A (left) and Pisces B (right) from pODI on WIYN. The images are $1'$ tall, N is up, and E is left.
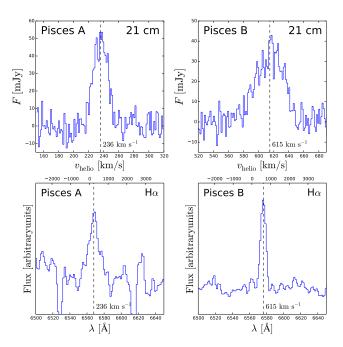

FIG. 2.— Spectra of the dwarf galaxies. The upper panels show the GALFA-HI spectra for the clouds near Pisces A (upper-left) and Pisces B (upper-right). The lower panels show the longslit optical spectra near Hα for Pisces A (lower-left) and Pisces B (lower-right). In all panels, the dashed black vertical lines are the emission features redshfited to 236 and 615 km s^{-1} for Pisces A and Pisces B, respectively. Both optical spectra show Hα emission at velocities consistent with the H I peak, confirming that the optical galaxies correspond to the H I clouds.

3. DISTANCES

TABLE 1
KEY OBSERVED PROPERTIES OF THE DWARF GALAXIES.

		Pisces A		Pisces B	
		Distance-independent Properties			
(1)	R.A. (J2000)	$00^h14^m46^s0$		$01^h19^m11^s7$	
(2)	Dec (J2000)	$+10°48'47''01$		$+11°07'18''22$	
(3)	l (°)	108.52		133.83	
(4)	b (°)	-51.03		-51.16	
(5)	m_r (mag)	17.35 ± 0.05		17.18 ± 0.07	
(6)	$(g-r)_0$ (mag)	0.17 ± 0.08		0.27 ± 0.1	
(7)	$R_{\mathrm{eff},r}$ (')	7.3 ± 0.2		5.6 ± 0.2	
(8)	P.A. (°)	111 ± 3		156 ± 1	
(9)	F_{HI} (Jy km s^{-1})	1.22 ± 0.07		1.6 ± 0.2	
(10)	M_{HI} ($10^5 M_\odot/D^2_{\mathrm{Mpc}}$)	2.8 ± 0.2		3.8 ± 0.4	
(11)	$v_{\mathrm{helio,HI}}$ (km s^{-1})	236 ± 0.5		615 ± 1	
(12)	$W50_{\mathrm{HI}}$ (km s^{-1})	22.5 ± 1.3		43 ± 3	
(13)	$v_{\mathrm{helio,opt}}$ (km s^{-1})	240 ± 34		607 ± 35	
(14)	f_{gas}	0.80 ± 0.02		0.84 ± 0.02	
		Distance-dependent Properties			
	Distance Scenario	Hubble flow	Nearby	Hubble flow	Nearby
(15)	D (Mpc)	3.5	1.7	8.9	3.5
(16)	M_r (mag)	-10.6	-9.0	-12.7	-10.7
(17)	$R_{\mathrm{eff},r}$ (pc)	123	60	241	95
(18)	M_* ($10^5 M_\odot$)	12.2	2.87	80.8	12.5
(19)	M_{HI} ($10^5 M_\odot$)	34.3	8.09	301	46.6
(20)	M_{tot} ($10^5 M_\odot$)	60.2	14.2	502	77.7

Rows (1) through (14) are properties that do not require an assumed distance. (1) through (4) provide the locations of the object in J2000 Equatorial and Galactic coordinates. Rows (5), (6), (7), and (8) are the r-band apparent magnitude, $g-r$ color (extinction corrected using the Schlafly & Finkbeiner 2011 correction to Schlegel et al. 1998), half-light radius (on-sky), and position angle (East of North). (9) is the total H I line flux, and (10) is the corresponding H I mass for a galaxy at 1 Mpc. Rows (11) and (12) are the central velocity and FWHM of the H I line from GALFA-HI, and (13) gives the central velocity of the Hα emission. (14) is the gas fraction $f_{\mathrm{gas}} = 1.4 M_{\mathrm{HI}}/M_{\mathrm{tot}}$ (see E.g. McGaugh 2012 for a discussion of the 1.4 factor). The remaining rows are properties that require an assumed distance (see Section 3 for a discussion of the scenarios), and the assumed distance is specified in Row (15). Rows (16) and (17) give r-band absolute magnitude and physical half-light radius. Row (18) gives the stellar mass, assuming $\frac{M_*/L_V}{M_\odot/L_\odot} \sim 1$ and (Jester et al. 2005) r- to V-band conversion. Row (19) is the H I mass, and (20) is the total mass ($M_* + 1.4 M_{\mathrm{HI}}$).
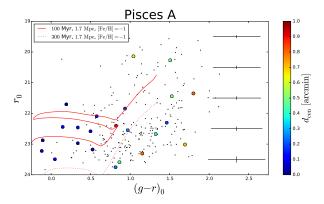

FIG. 3.— gr color-magnitude diagram for point sources near Pisces A. Colored circles are those within one arcminute (color indicates distance from the center of Pisces A), while black points are more distant. Typical error bars are shown on the right (including uncertainty from the unresolved diffuse component). The (red) lines show isochrones from Chen et al. (2014) with [Fe/H] = −1, $d = 1.7$ Mpc and ages of 100 Myr and 300 Myr for solid and dotted lines, respectively. While there is degeneracy between distance and age, the blueness of the stars indicate that at least a partially young population is necessary, and therefore a relatively close distance.

The basic details of the two objects described in Section 2 are summarized in Table 1. From these details and the morphology visible in Figure 1, it is clear that they are relatively nearby dwarf galaxies. In the imaging they are similar to the Leo P dwarf galaxy, also discovered

in H I. Pisces A in particular has a very similar H I line width as Leo P ($W_{50} \sim 25$ km s^{-1}), although both it and Pisces B are optically somewhat fainter than Leo P, while having similar 21 cm flux. Further comparisons require the answer to a crucial question: what is the distance to Pisces A and Pisces B? We consider this question for each galaxy in turn below.

3.1. Pisces A

We consider two scenarios for the distance to Pisces A. The first is, based on the assumption that Pisces A is in the Hubble flow. That is, its distance is simply $D = v/H_0 = 3.5$ Mpc. This case is considered in the first column of Table 1. In this scenario, Pisces A is not part of the Local Group, but nearby, well within the Local Volume.

Our second scenario is based on the presence of resolved stars in Pisces A (left panel of Figure 1). In Figure 3, we show the CMD of these resolved stars. While the colors have large uncertainty due to the diffuse light, the presence of a large number of blue point sources is suggestive of young main sequence stars. If we consider Leo P as a template for this galaxy, the brightest main sequence stars in Leo P are comparable in magnitude to the Pisces A stars (Rhode et al. 2013, using the color transformations of Jester et al. 2005). Hence, for our second distance scenario, detailed in the second column of Table 1, we assume a distance equal to that of Leo P (1.72 Mpc, McQuinn et al. 2013). Pisces A is relatively close in pro-

jection to M31, so in this scenario, $d_{M31} = 1.1$ Mpc. This is comparable to the Local Group's zero-velocity distance (~ 1.06 Mpc from McConnachie 2012), placing Pisces A just beyond the edge of the Local Group.

3.2. *Pisces B*

Pisces B has a higher radial velocity than Pisces A (615 km s^{-1} from the H I), yielding a larger distance in the Hubble flow scenario (8.9Mpc). In this case, Pisces B is still within the Local Volume, but somewhat more luminous than Leo P or Pisces A, possibly akin to a Blue Compact Dwarf (BCD). This is further suggested by its higher H I line width ($W_{50} \sim 45$ km s^{-1}). This scenario is considered in the third column of Table 1.

In the pODI imaging (right panel of 1), Pisces B appears to contain several potential point sources. However, Pisces B has more diffuse light than Pisces A, making it difficult to obtain accurate photometry and estimate a distance based on stellar CMDs. Additionally, the much stronger Hα emission apparent in Figure 2 (lower-right panel), as well as its detection in the UV with *GALEX* (FUV = 18.93, NUV = 18.87, Donovan Meyer et al., submitted), means that at least some of the brighter point sources may be unresolved H II regions rather than distinct stars. That said, if these point sources are resolved stars, it is possible that Pisces B is somewhat closer than the Hubble flow distance implies, and instead it has a substantially positive peculiar velocity. In the absence of deeper and higher-resolution imaging to resolve this question, in the fourth column of Table 1, we simply consider the *limiting* case that Pisces B is as close as the Hubble Flow scenario for Pisces A.

4. DISCUSSION AND CONCLUSIONS

In Figure 4, we show the two dwarf galaxies in the context of nearby dwarf galaxies. These include the Local Group dwarfs (as compiled in McConnachie 2012), the SHIELD sample of nearby $10^6 - 10^7 M_\odot$ H I-rich galaxies (Cannon et al. 2011), and Leo P. The upper panel demonstrates that, depending on the distance, the galaxies described here may be among the faintest known starforming galaxies. They also overlap in their basic structural properties with Local Group dwarfs, although they are somewhat more compact. Unlike the Local Group galaxies, however, they are well beyond the virial radii of any large dark matter halo like that of the MW or M31. Hence, they are crucial data points both for understanding how star formation functions at the lowest luminosities and as possible progenitors of the faint (predominantly passive) dwarf satellites of the Local Group.

Additionally, the lower panel of Figure 4 shows they have a slightly higher H I mass relative to typical dwarfs of the same luminosity. The resulting gas fractions (last row of Table 1), while high, are not necessarily surprising, as both the mean and scatter in gas fractions increase for fainter dwarfs (Geha et al. 2006, Bradford et al. in prep). Furthermore, these galaxies were discovered initially via H I, so detection biases favor higher H I masses. Nevertheless, the existence of a significant nearby population of faint galaxies with high H I content may offer significant constraints on dwarf galaxy formation models.

Motivated by the existence of these galaxies, we are identifying further candidate nearby, faint, starforming
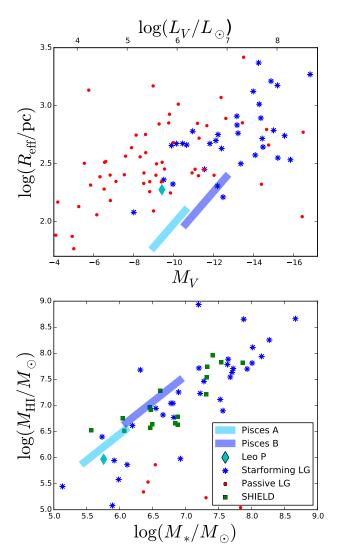

FIG. 4.— Upper panel: Comparison of Pisces A and Pisces B to nearby dwarf galaxies in size vs. luminosity. Lower panel: Comparison of Pisces A and Pisces B to nearby galaxies in stellar mass vs. H I mass. Local Group galaxy properties are from McConnachie (2012). Leo P properties are from McQuinn et al. (2013) (the size described there is for an outer detectable extent, and thus is an upper limit on $R_{\rm eff}$). The SHIELD sample of low-mass H I-rich nearby dwarfs is from Cannon et al. (2011). The shaded bars show the properties of Pisces A (cyan) and Pisces B (blue) between the two distance scenarios discussed in the text. For the upper panel, we use the Jester et al. (2005) transformations to convert from r-band magnitudes for Pisces A and Pisces B. For the lower panel, we make the estimate $\frac{M_*/L_V}{M_\odot/L_\odot} \sim 1$.

dwarfs in the SDSS. As discussed in Section 2.2, Pisces A and Pisces B have blue point sources in the SDSS catalog (although it mis-classifies them as galaxies due to the surrounding diffuse light). We conducted a search in the DR10 catalog for similar clusters of blue objects not associated with known galaxies or Galactic structures. While most such overdensities turn out to be artifacts, ~ 100 show morphologies potentially consistent with nearby dwarf galaxies. An ongoing spectroscopic follow-up campaign on these objects shows that some do indeed have Hα emission consistent with local galaxies, and we will present these results in a future paper.

4.1. *Comparison to Simulation*

Detailed use of these galaxies as data points for galaxy formation or evolution will require more firm distances, only possible with deeper and/or higher resolution photometry (which will be obtained by our approved Cycle 22 *Hubble Space Telescope* program). However, an initial interpretation is possible simply based on the detection of Pisces A in GALFA-HI and a comparison to a collisionless cosmological dark matter simulation. Specifically, we compare to the publicly available halo catalogs of the ELVIS suite (Garrison-Kimmel et al. 2014), considering only the "paired" simulations in ELVIS designed to resemble the Milky Way/M31 pairing of the real Local Group. We mock observe the dark matter halos from each of these pairs from a frame rotating at 220 km s^{-1} and 8 kpc from the center of each of the pairs. GALFA-HI can begin to distinguish high velocity cloud complexes from galaxy candidates around $v_{\mathrm{helio}} > 90$ km s^{-1} (Saul et al. 2012), so we only consider halos with corresponding mock v_{helio} values. We further sub-select only the halos *beyond* the host's virial radius (out to the edge of the ELVIS volumes, $d \lesssim 2\,\mathrm{Mpc}$), and with stellar masses[8] $10^5 < M_*/M_\odot < 10^8$. This yields 13 ± 4 halos, which we can compare to the observations.

The first data release of GALFA-HI covers 18% of the sky, so we expect of order $1 - 3$ galaxies to be found in GALFA-HI based on the above estimate of the number of ELVIS halos. There is one galaxy of the appropriate stellar mass and velocity in that range, Pisces A (the most likely distances for Pisces B place it beyond the edge of most of the ELVIS simulations), so there is at least not an order-of-magnitude discrepancy between the expectations of ΛCDM and the observations. While only one object, this also hints that because the number density of H I-selected faint dwarfs is roughly the same as that of corresponding ELVIS halos, even these low-mass halos typically have H I if they are beyond the Local Group.

4.2. *Conclusions*

The two new nearby dwarf galaxies we report here, discovered from their H I emission, provide new opportunities to study the faintest starforming galaxies. While detailed interpretation of the galaxies depends on the (uncertain) distance, rough estimates suggest broad consistency with ΛCDM. They also suggest that these galaxies could represent a larger population of nearby faint starforming dwarfs at the limits of detectability. These galaxies, and others like them, may thus provide a stepping stone from the dwarfs of the Local Group to the realm beyond.

REFERENCES

Ahn, C. P., Alexandroff, R., Allende Prieto, C., et al. 2014, ApJS, 211, 17
Astropy Collaboration, Robitaille, T. P., Tollerud, E. J., et al. 2013, A&A, 558, A33
Bertin, E., Mellier, Y., Radovich, M., et al. 2002, in Astronomical Society of the Pacific Conference Series, Vol. 281, Astronomical Data Analysis Software and Systems XI, ed. D. A. Bohlender, D. Durand, & T. H. Handley, 228
Boylan-Kolchin, M., Bullock, J. S., & Kaplinghat, M. 2011, MNRAS, 415, L40
Cannon, J. M., Giovanelli, R., Haynes, M. P., et al. 2011, ApJ, 739, L22
Chen, Y., Girardi, L., Bressan, A., et al. 2014, MNRAS, 444, 2525
Foreman-Mackey, D., Hogg, D. W., Lang, D., & Goodman, J. 2013, PASP, 125, 306
Garrison-Kimmel, S., Boylan-Kolchin, M., Bullock, J. S., & Lee, K. 2014, MNRAS, 438, 2578
Geha, M., Blanton, M. R., Masjedi, M., & West, A. A. 2006, ApJ, 653, 240
Geha, M., Brown, T. M., Tumlinson, J., et al. 2013, ApJ, 771, 29
Giovanelli, R., Haynes, M. P., Adams, E. A. K., et al. 2013, AJ, 146, 15
Grcevich, J. 2013, PhD thesis, Columbia University
Grcevich, J., & Putman, M. E. 2009, ApJ, 696, 385

Hargis, J. R., Willman, B., & Peter, A. H. G. 2014, ArXiv e-prints, arXiv:1407.4470
Hinshaw, G., Larson, D., Komatsu, E., et al. 2013, ApJS, 208, 19
Jester, S., Schneider, D. P., Richards, G. T., et al. 2005, AJ, 130, 873
Kirby, E. N., Guhathakurta, P., Simon, J. D., et al. 2010, ApJS, 191, 352
Klypin, A., Kravtsov, A. V., Valenzuela, O., & Prada, F. 1999, ApJ, 522, 82
Kravtsov, A. 2010, Advances in Astronomy, 2010, 281913
McConnachie, A. W. 2012, AJ, 144, 4
McGaugh, S. S. 2012, AJ, 143, 40
McQuinn, K. B. W., Skillman, E. D., Berg, D., et al. 2013, AJ, 146, 145
Moore, B., Ghigna, S., Governato, F., et al. 1999, ApJ, 524, L19
Peek, J. E. G., Heiles, C., Douglas, K. A., et al. 2011, ApJS, 194, 20
Pontzen, A., & Governato, F. 2012, MNRAS, 421, 3464
Rhode, K. L., Salzer, J. J., Haurberg, N. C., et al. 2013, AJ, 145, 149
Saul, D. R., Peek, J. E. G., Grcevich, J., et al. 2012, ApJ, 758, 44
Schlafly, E. F., & Finkbeiner, D. P. 2011, ApJ, 737, 103
Schlegel, D. J., Finkbeiner, D. P., & Davis, M. 1998, ApJ, 500, 525
Spekkens, K., Urbancic, N., Mason, B. S., Willman, B., & Aguirre, J. E. 2014, ApJ, 795, L5
Stetson, P. B. 1987, PASP, 99, 191

[8] Stellar masses in ELVIS were assigned via the abundance matching prescription of Garrison-Kimmel et al. (2014).

Strigari, L. E., Bullock, J. S., Kaplinghat, M., et al. 2008, Nature, 454, 1096

Tollerud, E. J., Bullock, J. S., Strigari, L. E., & Willman, B. 2008, ApJ, 688, 277

Walsh, S. M., Willman, B., & Jerjen, H. 2009, AJ, 137, 450